

See discussions, stats, and author profiles for this publication at: <https://www.researchgate.net/publication/231231427>

# CNT-Encapsulated $\beta$ -SiC Nanocrystals: Enhanced Migration by Confinement in Carbon Channels

ARTICLE *in* CRYSTAL GROWTH & DESIGN · MARCH 2011

Impact Factor: 4.89 · DOI: 10.1021/cg200065y

CITATIONS

13

READS

37

5 AUTHORS, INCLUDING:



**Mikhael Bechelany**

Université de Montpellier

**113** PUBLICATIONS **1,358** CITATIONS

SEE PROFILE



**Arnaud Brioude**

Claude Bernard University Lyon 1

**108** PUBLICATIONS **1,973** CITATIONS

SEE PROFILE



**Samuel Bernard**

Université de Montpellier

**106** PUBLICATIONS **1,250** CITATIONS

SEE PROFILE



**Philippe Miele**

Ecole Nationale Supérieure de Chimie de Mo...

**293** PUBLICATIONS **4,410** CITATIONS

SEE PROFILE

# CNT-Encapsulated $\beta$ -SiC Nanocrystals: Enhanced Migration by Confinement in Carbon Channels

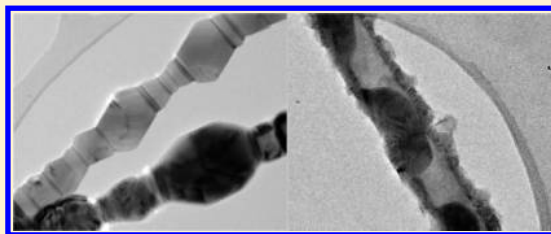
Mikhael Bechelany,<sup>\*,†</sup> Arnaud Brioude,<sup>‡</sup> Samuel Bernard,<sup>†</sup> David Cornu,<sup>†</sup> and Philippe Miele<sup>†</sup>

<sup>†</sup>Institut Européen des Membranes (UMR CNRS 5635), Université Montpellier 2, Place Eugène Bataillon, 34095 Montpellier, France

<sup>‡</sup>Laboratoire des Multimatériaux et Interfaces, UMR 5615 CNRS-Université Lyon 1, Université de Lyon, 43 bd du 11 novembre 1918, F-69622 Villeurbanne, France

**S** Supporting Information

**ABSTRACT:** Batch-fabricated SiC nanowires (NWs) and SiC@C nanocables (NCs) were heated under an argon flow at high temperature (1600–1800 °C). The ensuing product was characterized by SEM, HRTEM, EDX and XRD. As we found, the heat treatment led to the structuring of SiC NWs, whereas SiC@C NCs were completely converted into carbon nanotubes (CNTs) encapsulating faceted  $\beta$ -SiC nanocrystals. The growth mechanism of these nanostructures (NSs) was studied. The results collected in this study will enable us to better define use conditions of SiC-based 1D NSs at high temperatures and to understand the effect of confinement on the migration of element during annealing. These NSs could have applications in different fields such electronic and light-emitting diode.



## INTRODUCTION

Since the observation of carbon nanotubes (CNTs) by Iijima in 1991,<sup>1</sup> an increasing number of works has been devoted these two last decades to the synthesis and applications of this type of nanostructure (NS). Among the wide number of studies, the ability to fill the inner cavities of CNTs with a wide variety of materials (Ag,<sup>2</sup> Ni,<sup>3</sup> Co,<sup>4</sup> C60,<sup>5</sup> Se, S, Sb, and Ge<sup>6</sup>) was extensively investigated. Besides, cubic silicon carbide ( $\beta$ -SiC) NSs have attracted interests according to their chemical and physical properties that are more interesting than those of CNTs in particular for thermostructural applications. Indeed, SiC is a wide band gap semiconducting material that exhibits outstanding properties, such as high thermal and chemical stabilities, high hardness, and high mechanical strength. These excellent physical and chemical properties make SiC a good candidate not only for thermostructural applications but also for microelectronic devices designed for high-temperature, high-power, and high-frequency applications.<sup>7–9</sup> Within this context, the synthesis of SiC-based nanowires (NWs) and nanocables (NCs) has attracted much attention for their possible applications as catalyst supports,<sup>10</sup> reinforcement materials in nanocomposites,<sup>11</sup> components for nanoelectronic device<sup>12</sup> or for nanoelectromechanical systems.<sup>13</sup> Herein, we focused on the combination of the properties of carbon and  $\beta$ -SiC in one nanomaterial. This combination has never been reported, i.e., synthesis of CNTs with SiC nanocrystals. This may lead to novel nanomaterials with important applications in nanotechnology, such as nanoscale multiterminal electronic devices and light-emitting diode,<sup>14</sup> and can improve the physical (mechanical and electrical) properties of the obtained nanomaterials.

Recently, we developed a simple procedure for large-scale production of pure SiC-based NWs and coaxial NCs from low-

cost reagents.<sup>15</sup> These SiC-based 1D NSs exhibit valuable physical properties.<sup>16–19</sup> Indeed, high mechanical performances have been demonstrated for these SiC-based NWs and NCs in term of Young modulus ( $\sim 500$  GPa)<sup>17</sup> and quality factor ( $Q \approx 150\,000$ ).<sup>17</sup> Raman spectroscopy investigations tend to support a p-type doping of these NSs with an estimated free carrier concentration between  $1 \times 10^{18}$  and  $1 \times 10^{19}$  cm<sup>-3</sup>.<sup>20</sup> Because of the envisaged high-temperature applications of these nanomaterials, we recently started to study their chemical and structural stability at high temperature under different atmospheres. As an illustration, the heat treatment under ammoniac at 1400 °C converted the SiC NWs into Si<sub>3</sub>N<sub>4</sub> nanorods.<sup>21</sup> A simple dry-air thermal treatment up to 550 °C transformed SiC@C NCs into SiC@SiO<sub>2</sub> NCs.<sup>22</sup> In the present paper, we use these SiC NWs and coaxial NCs as precursors of new varieties of SiC-based NSs. By a simple annealing treatment at high temperature, we demonstrate the possibility to prepare a new geometry of SiC NWs, i.e., faceted SiC NWs as well as the synthesis of CNTs filled with faceted  $\beta$ -SiC nanocrystals. The study of these new morphologies allows us to understand the migration enhancement of SiC inside the channels of the formed CNTs and to control their synthesis. The high yield synthesis of these NSs is of main importance for the investigations of their physical and chemical properties.

## EXPERIMENTAL SECTION

All the NSs depicted in this paper were analyzed by the means of scanning electron microscopy (SEM, Model S800, Hitachi),

**Received:** January 17, 2011

**Revised:** February 18, 2011

**Published:** March 08, 2011

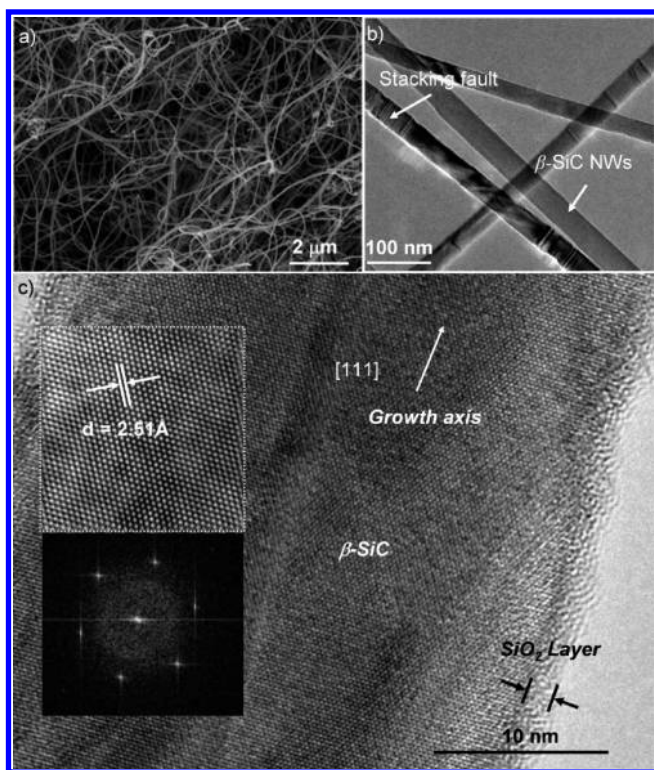


**Figure 1.** (a) SEM image of the as-grown SiC NWs, (b) Conventional TEM image; stacking faults are marked by the white arrows, (c) HRTEM image of a NW of 40 nm in diameter; the associated calculated Fourier transform in inset.

high-resolution transmission electron microscopy (HRTEM, TOP-CON 002B), energy-dispersive X-ray spectroscopy (EDX, KEVEX SIGMA, NORAN Instruments), and XRD analysis using a Philipps PW 3040/60 X'Pert PRO X-ray diffraction system (Cuka radiation;  $\lambda = 1.5406 \text{ \AA}$  at 40 kV and 30 mA). Samples of pure intermixed SiC based NWs were used as starting materials. Such materials were prepared by a vapor-solid (VS) growth mechanism and according to a procedure described elsewhere.<sup>15</sup>

**Annealing of 1D SiC-Based NSs.** In a typical experiment, a carbon boat filled with 100 mg of SiC NWs or SiC@C NCs was placed into a graphitic furnace (Gero Model HTK 8). The furnace was heated under an argon flow ( $10 \text{ L h}^{-1}$ ) up to 1800 or 1600 °C successively (heating rate  $200 \text{ °C h}^{-1}$ ). The temperature was maintained for 2 h then allowed to cool down to room temperature. Finally,  $\sim 100 \text{ mg}$  of as-obtained sample was removed from the carbon boat and fully characterized.

## RESULTS AND DISCUSSION

**Synthesis of Faceted SiC NWs.** In a preliminary experiment, a felt of NWs consisting in an isotropic 3D network of intermixed pure SiC NWs was prepared according to an established experimental procedure.<sup>15</sup> The XRD pattern of as-obtained samples is presented in Figure S1 in the Supporting Information. The XRD pattern indicates that the raw product contains the cubic polytype of SiC ( $\beta$ -SiC) (JCPDS Card No. 29-1129). SEM investigations (Figure 1a) show that the crude product is only made of interlaced NWs, with no trace of any residual particles. The SiC NWs exhibited diameter of  $\sim 40 \text{ nm}$  for lengths up to several hundreds of micrometers. Low-magnification TEM image (Figure 1b) illustrates the homogeneity in diameters of the SiC NWs with values falling in the range 30–40 nm. Some

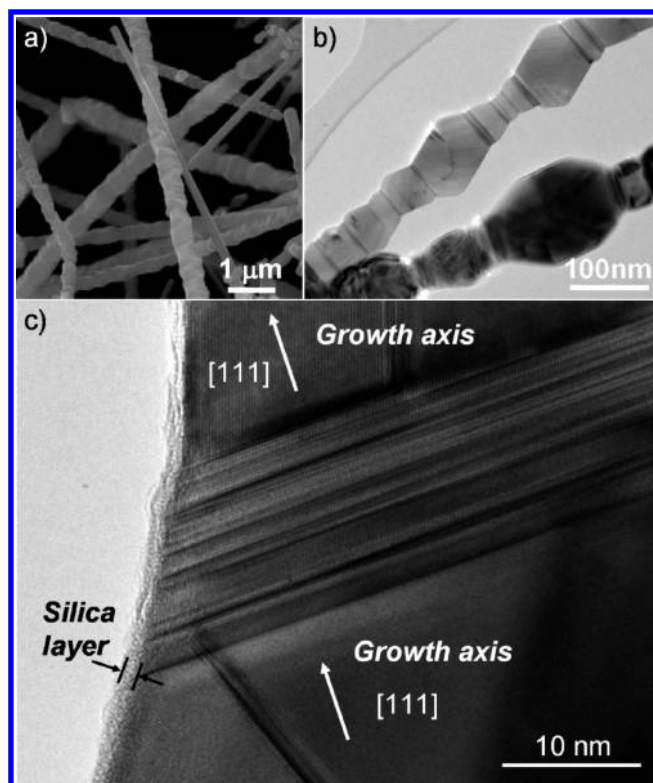


**Figure 2.** (a) SEM image of the SiC NWs heated at 1800 °C; (b) TEM image in the conventional mode; and (c) HRTEM image of a single NW.

stacking-faults (SFs) aggregations, marked with a white arrow on figure 1b, are randomly observed along the NWs. Figure 1c shows the HRTEM image of a NW of 40 nm in diameter representative of the sample. This image illustrates that this NW has a homogeneous crystalline structure with fringes resolved at  $2.51 \text{ \AA}$ , which is characteristic of  $\beta$ -SiC. The growth direction is parallel to the  $[111]$  crystallographic direction. We also note the presence of a thin layer of  $\text{SiO}_2$  with a regular thickness of 2 nm formed upon exposition to air. In a previous work,<sup>20</sup> we have focused our efforts on the correlation between the high-resolution transmission electron microscopy (HRTEM) images, the Raman spectral profiles of single 3C-SiC NWs, and their SFs. These studies showed both atomic arrangements in the SiC NWs with growth predominantly in the  $[111]$  direction and abundant structural defects. The SF density varied as the function of the diameter of SiC NWs. This observation makes very difficult the quantification of these SFs.

The SiC NWs were annealed at 1800 °C under argon to produce a new variety of SiC NSs with particular properties. SEM images of the annealed SiC NWs reported in Figure 2a revealed a deep modification in their morphology whereas EDX measurements combined with SEM and TEM observations indicated that the SiC NWs do not undergo any chemical changes. An increase of the roughness of the surface of SiC NWs is observed. The NWs diameter becomes higher and heterogeneous over their length. These diameters lie between 10 and 300 nm but are mainly lower than 60 nm. The presence of elbows along the NWs makes difficult the measurement of their lengths which can nevertheless be considered higher than  $100 \text{ }\mu\text{m}$ . The NWs lose their flexibility and became very linear. TEM observations (Figure 2b,c) showed that the NSs always consist of cubic silicon



carbide. The image obtained in conventional mode (Figure 2b) confirmed the heterogeneity in diameter. Figure 2c shows a  $\beta$ -SiC NW with 50 nm diameter approximately and presenting an angle. The geometrical characteristics of the angles were examined more in detail by HRTEM. This study shows that this angle is based on the strong density of SFs domains but any growth direction change has been observed.

We assume that the heat treatment of the SiC NWs under argon at 1800 °C only leads to the reorganization of their morphology most probably caused by the Si (s) and C (s) atoms mobility at high temperature on the NWs surface. The elements migrate from the surface of the domains with strong density of defects toward the single-crystal domains. This phenomenon induces the diameter reduction on the level of the SFs aggregations and increases the diameter of the single-crystal domains. This clearly results in both the variation in the NW diameter and the appearance of marked angles between the two single-crystal domains. A sublimation of the Si and C elements then a condensation in the single-crystal domains cannot be excluded. A first step of this faceting is certainly the evaporation of the silica thin coating. After the thermal treatment, the presence of a silica layer with a regular thickness of 2 nm on the surface of the NWs (Figure 2c) is attributed to an oxidation of the SiC upon exposition to air. Moreover, it is interesting to note that no graphitization has been observed on the surface of the NWs (i.e., formation of a carbon coating) by the preferential sublimation of SiC via the formation of  $\text{Si}_2\text{C}$  gas species, as that is often observed on the single crystals surface of SiC at these temperatures and under argon.<sup>23</sup> This difference between the “bulk” and the NWs can be attributed to the role of evaporated  $\text{SiO}_2$ . Indeed,  $\text{SiO}(\text{g})$  present in the furnace atmosphere in considerable quantity taking into account the important specific surface of our nano-objects, is likely to react with the carbon on the SiC surface, thus leading to the formation of SiC and avoiding graphitization of a carbon layer. More experiments are in progress in order to better understand the influence of diameters and temperatures on these structuring of SiC NWs. We note here that the density of SFs in NWs is higher after annealing (Figure 2b). Chung et al.<sup>24</sup> already reported that SFs occurred during annealing of cubic SiC under Argon atmosphere. One of the mechanism suggested that SFs can form spontaneously in SiC because the crystal can lower its energy. Therefore we suggest that the higher density of SFs observed after annealing could be attributed to the minimizing of surface energy. The SFs have a significant influence on the physical (mechanical and electrical) properties of nanowires. As reported before, these SFs could be attributed to other SiC polytypes. Experiments are in progress in order to isolate individual structured SiC NWs and study their physical properties.<sup>20</sup> In parallel, we intend to incorporate these NWs in polymer matrix,<sup>18</sup> for instance, in order to investigate their collective properties. Such nanomaterials could have applications in different fields because high-energy crystal surfaces usually exhibit fascinating surface-enhanced properties and have promising applications in catalysis, photoelectrical devices, and energy conversion.<sup>25</sup>

**Growth of CNTs Filled with Faceted  $\beta$ -SiC Nanocrystals.** In a preliminary experiment, a felt of NWs consisting in an isotropic 3D network of intermixed pure SiC@C NCs was prepared according to an established experimental procedure.<sup>15</sup> The XRD pattern of as-obtained samples is presented in Figure S2 in the Supporting Information. The XRD pattern indicates that the raw product contains the cubic polytype of SiC ( $\beta$ -SiC)

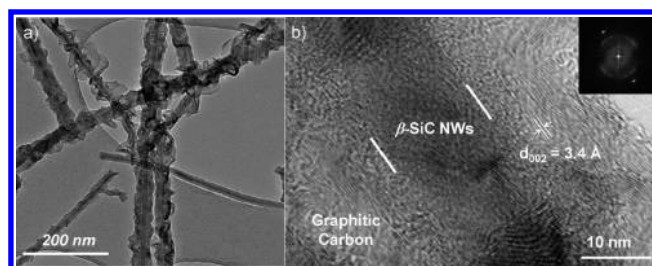


**Figure 3.** (a) Conventional TEM image of the as-grown SiC@C NCs, (b) HRTEM image of a NC of 70 nm in diameter, and associated calculated Fourier transform in inset.

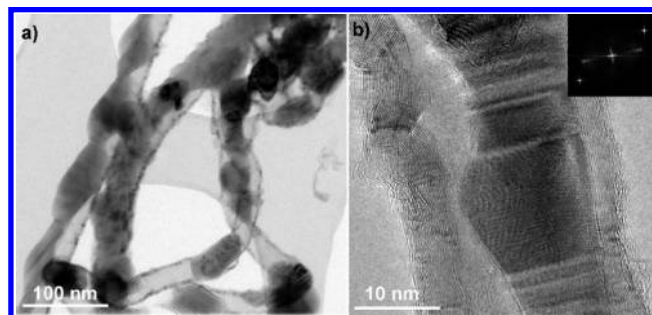


**Figure 4.** (a) TEM image in the conventional mode of the SiC@CNTs, (b) HRTEM image of a NS of 30 nm in diameter; associated calculated Fourier transform in inset.

(JCPDS Card No. 29–1129). Moreover we identify peaks at  $2\theta = 26.4$ ,  $\sim 43$ , and  $54.5^\circ$  that we attributed to the (002), (10), and (004) peaks diffraction of graphitic carbon. The reflection (002) of this carbon is not very intense, asymmetric, and sprawled over several degrees, what indicates a certain proportion of disorder in the structure. We deduce that is characterized by a two-dimensional structure similar to a turbostratic structure. This could be also attributed to a size effect. SEM images showed that the SiC based 1D NSs exhibited diameter of  $\sim 50$  nm for lengths up to several hundreds of micrometers. Low magnification TEM image (Figure 3a) revealed the heterogeneity in diameters along these SiC NCs with values falling in the range 50–80 nm. Figure 3b shows the HRTEM image of a NC of 70 nm in diameter representative of the sample. It consists of a SiC core of  $\sim 20$  nm in diameter covered by a carbon coating of  $\sim 10$ –20 nm in thickness. This turbostratic structure of graphite was confirmed on the basis of its evaluated  $d_{002}$  interplanar distance ( $3.4 \text{ \AA}$ )<sup>26</sup> on the HRTEM image (Figure 3b) which is slightly superior to the theoretical value in graphite ( $3.36 \text{ \AA}$ , JCPDS Card No. 00–001–0640). These graphitic planes were found to be not always oriented along the NW axis.

After heat treatment of the SiC@C felt under argon at 1600 °C, SEM images (see Figure S3 in the Supporting Information) and EDX measurement performed during SEM and TEM observations did not show any chemical changes. The XRD pattern shows that the reflection (002) of this carbon remains poorly intense, asymmetric and sprawl over several degrees. That could be also attributed to a size effect. Moreover, Figure 4 showed a deep morphological change of these SiC@C NCs. The core of cubic silicon carbide started to recrystallize to give shapes similar to those described in the first part. The carbon was graphitized to give concentric planes of structure very close to

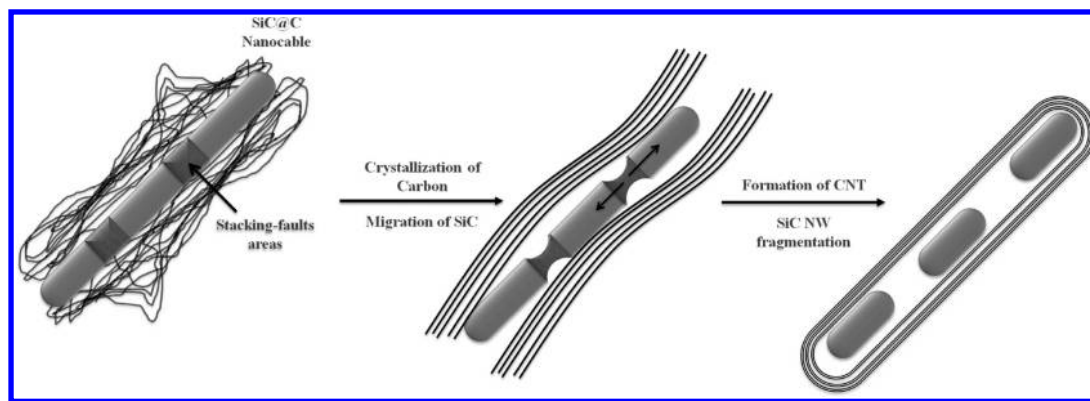
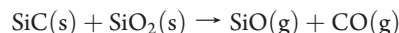


**Figure 5.** Schematic process of the synthesis of CNTs encapsulating SiC nanocrystals.

that of the multiwall carbon nanotubes (MWCNTs) (Figure 4b). We can clearly distinguish the orientation of the carbon planes (002) along the NCs axis. The heat treatment of SiC@C NCs leads thus to the formation of SiC@CNTs, consisting of MWCNTs encapsulating SiC single crystals. These 1D NSs lose their flexibility and we can observe elbows along the NSs. The SiC nanocrystals are randomly distributed inside the MWCNTs and TEM observations (see Figure S4 in the Supporting Information) shows that the ends of the CNTs are closed. Filling CNTs by SiC nanomaterials has not been reported before. This result is very important because the studies showed that the structural modification generated by confinement inside the channel of CNTs has an influence on the materials properties. The possibility of synthesizing new nanomaterials with exceptional properties appeared.<sup>27–30</sup> It will give the possibility to study the properties of SiC nanocrystals encapsulated into CNTs. Such new materials extend the applications of CNTs in new fields of nanotechnology, such as nanoscale multiterminal electronic devices and light-emitting diode.<sup>14</sup>

**Enhanced Migration by Confinement in Carbon Channels.** The schematic process of the formation of these NSs is shown in Figure 5. We know that when we bring SiC NWs at high temperature (Figure 2), reorganization occurs leading to the transfer (by migration or sublimation) of the atoms from the domains of strong density of stacking fault toward the single-crystal domains. In our experiment, the starting product consists of SiC@C NCs. Under the effect of the heat treatment, the carbon coating crystallizes. Reinforced by a template effect of the SiC NWs cores, this crystallization led to the formation of cylindrical MWCNTs, without strong chemical link with the SiC core. The last behave in the same way of that we saw in the last part: transfer of the atoms, probably by migration due to the high mobility of the surface from the domains with high density of stacking fault toward the single-crystal domains. This transfer leads to a total consumption of the domains with strong density of defects and to the formation of cubic SiC single crystals distributed randomly within MWCNTs. The difference in the kinetics of the atoms transfer in this experiment compared to the experiment with SiC NWs without coating, nevertheless carried at higher temperature (1800 °C instead of 1600 °C) during the same time, can be due to a confinement effect inside the channel of CNTs. This confinement effect implies probably a greater mobility of the atoms into the CNTs than in the processing atmosphere, undoubtedly because of the absence of interaction with any gas phase. The enhancement of atoms migration by confinement in CNTs channel has not been studied before. More

experiments are in progress in order to better understand the effect of temperature and time on the migration of SiC. The morphology of these obtained NSs remind that of NCs of the same type synthesized by the group of Bando in 2004, by thermal treatment at 1600 °C under ultrahigh vacuum of SiC@SiO<sub>2</sub>@C NCs prepared by VLS starting from Fe nanoparticles.<sup>31</sup> In the case of Bando, it is not continuous CNTs, since the diameter of SiC crystals is higher than that of CNTs. They are thus SiC crystals connected between them by bridges of CNTs. The authors proposed that these discontinuous nanostructures result from the two following competing reactions occurring at random along the nanowires:



The authors indicated that the first reaction yield to the formation of “CNTs bridges” domains and that the second reaction is responsible to the formation of the “wide SiC crystals” domains. Even if the morphology of our nanostructures is very close, we do not share the same analysis as the Bando group on the growth mechanism because their NSs are not pure (presence of iron catalyst) and are treated under vacuum.

A major challenge in the preparation of such nanocomposites is the effect of the diameter and the nature of the NTs on the SiC migration. For instance, using boron nitride NTs<sup>32</sup> or NTs with different diameters, we expect a different behavior. These opportunities are now being addressed, it is anticipated that this will lead to host of structural and functional applications for a new generation of nanomaterials.

## CONCLUSION

In summary, the thermal treatment of SiC NWs and SiC@C NCs under argon has been realized at high temperature (1600–1800 °C). As we found, the heat treatment induces the structuring of SiC NWs, whereas SiC@C NCs were completely converted into CNTs filled by faceted  $\beta$ -SiC nanocrystals. The growth mechanism of these nano-objects was studied and the enhancement of the migration of atoms inside the channel of CNTs was analyzed. This process has been influenced by the presence of a high-density of SFs areas in the initial SiC NWs and the formation of new SFs domains during annealing. The results collected in this study will enable us to better define use conditions of SiC-based NWs at high temperatures according to the processing atmosphere. It will also open the possibility to

study the physical and chemical properties of faceted SiC NWs and of SiC nanocrystals encapsulated into the channel of CNTs.

## ■ ASSOCIATED CONTENT

**S Supporting Information.** Additional figures (PDF). This material is available free of charge via the Internet at <http://pubs.acs.org/>.

## ■ AUTHOR INFORMATION

### Corresponding Author

\*Phone: +33467149181. Fax: +33467149119. Mikhael.Bechelany@iemm.univ-montp2.fr.

## ■ ACKNOWLEDGMENT

We gratefully acknowledge the CT $\mu$  (Centre Technologique des Microstructures) of the Université Lyon 1 for access to the SEM, the platform “Nanofils et Nanotubes de Lyon” and Dr. Gabriel Ferro for the scientific discussion.

## ■ REFERENCES

- (1) Iijima, S. *Nature* **1991**, 354, 56–58.
- (2) Ugarte, D.; Chatelain, A.; deHeer, W. A. *Science* **1996**, 274, 1897–1899.
- (3) Tessonier, J. P.; Ersen, O.; Weinberg, G.; Pham-Huu, C.; Su, D. S.; Schlogl, R. *ACS Nano* **2009**, 3, 2081–2089.
- (4) Sinha, A. K.; Hwang, D. W.; Hwang, L. P. *Chem. Phys. Lett.* **2000**, 332, 455–460.
- (5) Smith, B. W.; Monthieux, M.; Luzzi, D. E. *Nature* **1998**, 396, 323–324.
- (6) Loiseau, A.; Pascard, H. *Chem. Phys. Lett.* **1996**, 256, 246–252.
- (7) Han, W. Q.; Fan, S. S.; Li, Q. Q.; Liang, W. J.; Gu, B. L.; Yu, D. P. *Chem. Phys. Lett.* **1997**, 265, 374–378.
- (8) Zhou, X. T.; Zhang, R. Q.; Peng, H. Y.; Shang, N. G.; Wang, N.; Bello, I.; Lee, C. S.; Lee, S. T. *Chem. Phys. Lett.* **2000**, 332, 215–218.
- (9) Wong, K. W.; Zhou, X. T.; Au, F. C. K.; Lai, H. L.; Lee, C. S.; Lee, S. T. *Appl. Phys. Lett.* **1999**, 75, 2918–2920.
- (10) Zhu, S. M.; Xi, H. A.; Li, Q.; Wang, R. D. *J. Am. Ceram. Soc.* **2005**, 88, 2619–2621.
- (11) Yang, W.; Araki, H.; Tang, C. C.; Thaveethavorn, S.; Kohyama, A.; Suzuki, H.; Noda, T. *Adv. Mater.* **2005**, 17, 1519–1523.
- (12) Pan, Z. W.; Lai, H. L.; Au, F. C. K.; Duan, X. F.; Zhou, W. Y.; Shi, W. S.; Wang, N.; Lee, C. S.; Wong, N. B.; Lee, S. T.; Xie, S. S. *Adv. Mater.* **2000**, 12, 1186–1190.
- (13) Cambaz, G. Z.; Yushin, G. N.; Gogotsi, Y.; Lutsenko, V. G. *Nano Lett.* **2006**, 6, 548–551.
- (14) Xi, G. C.; Yu, S. J.; Zhang, R.; Zhang, M.; Ma, D. K.; Qian, Y. T. *J. Phys. Chem. B* **2005**, 109, 13200–13204.
- (15) Bechelany, M.; Brioude, A.; Stadelmann, P.; Ferro, G.; Cornu, D.; Miele, P. *Adv. Funct. Mater.* **2007**, 17, 3251–3257.
- (16) Ayari, A.; Vincent, P.; Perisanu, S.; Choueib, M.; Gouttenoire, V.; Bechelany, M.; Cornu, D.; Purcell, S. T. *Nano Lett.* **2007**, 7, 2252–2257.
- (17) Perisanu, S.; Gouttenoire, V.; Vincent, P.; Ayari, A.; Choueib, M.; Bechelany, M.; Cornu, D.; Purcell, S. T. *Phys. Rev. B* **2008**, 77, 165434.
- (18) Guiffard, B.; Guyomar, D.; Seveyrat, L.; Chowanek, Y.; Bechelany, M.; Cornu, D.; Miele, P. *J. Phys. D: Appl. Phys.* **2009**, 42, 055503.
- (19) Rogdakis, K.; Bano, E.; Montes, L.; Bechelany, M.; Cornu, D.; Zekentes, K. In *Silicon Carbide and Related Materials Pts 1 and 2*; Bauer, A. J., Friedrichs, P., Krieger, M., Pensl, G., Rupp, R., Seyller, T., Eds.; Trans Tech Publications Ltd: Stafa-Zurich, 2009; Vol. 645–648, pp 1235–1238.
- (20) Bechelany, M.; Brioude, A.; Cornu, D.; Ferro, G.; Miele, P. *Adv. Funct. Mater.* **2007**, 17, 939–943.
- (21) Bechelany, M.; Brioude, A.; Bernard, S.; Ferro, G.; Cornu, D.; Miele, P. *Nanotechnology* **2007**, 18, 335305.
- (22) Bechelany, M.; Cornu, D.; Chassagneux, F.; Bernard, S.; Miele, P. *J. Optoelectron. Adv. Mater.* **2006**, 8, 638–642.
- (23) Younes, G.; Ferro, G.; Jacquier, C.; Dazord, J.; Monteil, Y. *Appl. Surf. Sci.* **2003**, 207, 200–207.
- (24) Chung, H. J.; Liu, J. Q.; Skowronski, M. *Appl. Phys. Lett.* **2002**, 81, 3759–3761.
- (25) Jiang, Z. Y.; Kuang, Q.; Xie, Z. X.; Zheng, L. S. *Adv. Funct. Mater.* **2010**, 20, 3634–3645.
- (26) Niederberger, M.; Muhr, H. J.; Krumeich, F.; Bieri, F.; Gunther, D.; Nesper, R. *Chem. Mater.* **2000**, 12, 1995–2000.
- (27) Ajayan, P. M.; Iijima, S. *Nature* **1993**, 361, 333–334.
- (28) Ajayan, P. M.; Stephan, O.; Redlich, P.; Colliex, C. *Nature* **1995**, 375, 564–567.
- (29) Sloan, J.; Friedrichs, S.; Meyer, R. R.; Kirkland, A. I.; Hutchison, J. L.; Green, M. L. H. *Inorg. Chim. Acta* **2002**, 330, 1–12.
- (30) Meyer, R. R.; Sloan, J.; Dunin-Borkowski, R. E.; Kirkland, A. I.; Novotny, M. C.; Bailey, S. R.; Hutchison, J. L.; Green, M. L. H. *Science* **2000**, 289, 1324–1326.
- (31) Li, Y. B.; Bando, Y.; Golberg, D. *Adv. Mater.* **2004**, 16, 93–101.
- (32) Bechelany, M.; Brioude, A.; Stadelmann, P.; Bernard, S.; Cornu, D.; Miele, P. *J. Phys. Chem. C* **2008**, 112, 18325–18330.